INTERNATIONAL JOURNAL FOR NUMERICAL METHODS IN FLUIDS, VOL. 13, 425–436 (1991)

NUMERICAL SOLUTION OF 2D AND 3D TURBULENT INTERNAL FLOW PROBLEMS

CHEN NAIXING AND XU YANJI

Institute of Engineering Thermophysics, P.O. Box 2706, Beijing 100080, China

SUMMARY

The paper describes a method for solving numerically two-dimensional or axisymmetric, and three-dimensional turbulent internal flow problems. The method is based on an implicit upwinding relaxation scheme with an arbitrarily shaped conservative control volume. The compressible Reynolds-averaged Navier–Stokes equations are solved with a two-equation turbulence model. All these equations are expressed by using a non-orthogonal curvilinear co-ordinate system. The method is applied to study the compressible internal flow in modern power installations. It has been observed that predictions for two-dimensional and three-dimensional channels show very good agreement with experimental results.

KEY WORDS Numerical computation Internal flow Turbulent flow Turbomachinery Axisymmetric diffuser

INTRODUCTION

In modern power installations the flow phenomena that exist in advanced turbomachinery are extremely complex and propose a challenge to engineers and scientists to improve the design procedure. Such flows are generally unsteady, turbulent and three-dimensional. The viscous and turbulent effects have a substantial influence on properties of internal flow components. The appearance of secondary flows and boundary layer separations may bring about high energy losses.[1–3] Hence much more careful design is required, especially for decelerated internal flow. In the past decade, many efforts have been made to promote the efficiency of turbomachinery. Various aerodynamic computational methods[4–13] have been developed.

With the numerous analyses of inviscid numerical calculations it is difficult to obtain information on energy losses and boundary layer separations due to viscous effects. The rapid progress of high-speed computers and the considerable improvement in measuring techniques have stimulated the development of numerical calculations of the compressible viscous flow fields through turbomachinery cascades. It is urgent to develop a computational technique which can solve the two-dimensional and three-dimensional Reynolds-averaged Navier–Stokes equations in a practical CPU time. However, it is well known that the difficulty in solving the velocity is that the pressure distribution cannot be known beforehand or directly evaluated from the continuity equation. In 1972 the pressure correction method was developed by Patankar and Spalding.[14] In their paper the pressure correction method was first used for correcting the velocity distribution instead of satisfaction of the continuity equation, and a staggered grid system was employed to avoid the associated pressure and velocity oscillation efficiently. Since 1972 a series of papers[15–19] concerning the method of Patankar and Spalding have been successfully applied to predict the viscous flow fields and heat transfer characteristics in engineering practice.

0271–2091/91/140425–12$06.00

Received March 1990
Revised September 1990

On the basis of the above-described method, a set of governing equations of the compressible turbulent flow, expressed by using a non-orthogonal curvilinear co-ordinate system and physical contravariant components of vectors,[20] are applied in the present study and solved by a time-dependent technique and an implicit scheme with a conservative control volume. The purpose of this paper is to attempt to develop and assess a computer programme for the calculation of two-dimensional or axisymmetric, and three-dimensional turbulent internal flows. To obtain accurate numerical solutions for the complex turbulent flow, a two-equation turbulence model[21,22] is employed.

The governing equations and the turbulence model are described in the following section. The next section concentrates on the numerical procedure. Then a special computational grid system, namely an equiproportional grid system, is presented. For verification of the method, several numerical examples have been carried out and compared with experimental results. Conclusions resulting from the present study are given in the last section.

GOVERNING EQUATIONS AND TURBULENCE MODEL

The vector forms of the conservative equations describing the viscous flow[23] are written as follows:

continuity equation

$$\frac{\partial \rho}{\partial t}+\nabla\cdot(\rho\mathbf{V})=0, \tag{1}$$

momentum equation

$$\frac{\mathrm{d}\mathbf{V}}{\mathrm{d}t}=-\frac{1}{\rho}\nabla p+\frac{\mathbf{F}_{\mathrm{vis}}}{\rho}, \tag{2}$$

energy equation

$$\frac{\mathrm{d}I}{\mathrm{d}t}=\frac{1}{\rho}\frac{\partial p}{\partial t}+\dot{q}+\frac{1}{\rho}\mathbf{V}\cdot\mathbf{F}_{\mathrm{vis}}+\frac{\Phi}{\rho}, \tag{3}$$

where $\mathbf{V}$ is the absolute velocity vector, ρ, p and T denote the static density, pressure and temperature respectively, I represents the total enthalpy, $\mathbf{F}_{\mathrm{vis}}$ and $\mathbf{V}\cdot\mathbf{F}_{\mathrm{vis}}$ represent the viscous force vector and its work done respectively, Φ is the dissipation function and $\dot{q}$ denotes the heat transfer term.

Besides the above-mentioned equations the following equations are also employed:

definition of total enthalpy

$$I=C_{\mathrm{p}}T+V^2/2, \tag{4}$$

equation of a perfect gas

$$p=\rho RT. \tag{5}$$

The governing differential equations applied to the present study are the Reynolds-averaged Navier–Stokes equations of a compressible fluid. The viscous terms and heat transfer term are calculated from the effective viscosity and the effective conductivity respectively. They can be expressed as

$$\mu_{\mathrm{ef}}=\mu_{\mathrm{l}}+\mu_{\mathrm{t}}, \qquad \lambda=C_{\mathrm{p}}\left(\frac{\mu_{\mathrm{l}}}{Pr}+\frac{\mu_{\mathrm{t}}}{Pr_{\mathrm{t}}}\right), \tag{6}$$

where the laminar viscosity μ_l is determined from the thermal properties of the fluid and the turbulent viscosity μ_t is obtained by the expression

$$\mu_t = C_\mu \rho k^2/\varepsilon. \tag{7}$$

In the above equation C_μ is a constant, $C_\mu = 0{\cdot}09$. The turbulent kinetic energy k and its dissipation rate ε are predicted from a two-equation turbulence model. The governing differential equations for k and ε are

$$\frac{\partial(\rho k)}{\partial t} + \frac{1}{\sqrt{g}}\frac{\partial}{\partial x^j}\left((\sqrt{g})\rho v^j k - (\sqrt{g}) g^{jk}\frac{\mu_t}{\sigma_k}\frac{\partial k}{\partial x^k}\right) = G - \rho\varepsilon, \tag{8}$$

$$\frac{\partial(\rho \varepsilon)}{\partial t} + \frac{1}{\sqrt{g}}\frac{\partial}{\partial x^j}\left((\sqrt{g})\rho v^j \varepsilon - (\sqrt{g}) g^{jk}\frac{\mu_t}{\sigma_\varepsilon}\frac{\partial \varepsilon}{\partial x^k}\right) = \frac{\varepsilon}{k}(C_1 G - C_2\rho\varepsilon), \tag{9}$$

where G denotes the generation rate of turbulent kinetic energy and the empirical constants σ_k, σ_ε, C_1 and C_2 are set to the following values:

$$\sigma_k = 1{\cdot}0, \qquad \sigma_\varepsilon = 1{\cdot}3, \qquad C_1 = 1{\cdot}44, \qquad C_2 = 1{\cdot}92. \tag{10}$$

GENERALIZED FORM OF THE GOVERNING EQUATIONS

To handle the arbitrarily shaped boundaries conveniently, the continuity equation, momentum equations in three directions, energy equation and two equations of turbulence modelling are written in a general form and expressed by a curvilinear co-ordinate system:

$$\frac{\partial[\rho(\sqrt{g})\varphi]}{\partial t} + \frac{\partial}{\partial x^j}[\rho(\sqrt{g})v^j\varphi] = \frac{\partial}{\partial x^j}\left(\Gamma g^{jk}\frac{\partial\varphi}{\partial x^k}\right) + S_\varphi, \tag{11}$$

where

$$\varphi = [1, V_r, rV_\phi, V_z, I, k, \varepsilon]^{-1}, \tag{12}$$

$$\Gamma = [0, \mu_{ef}\sqrt{g}, \mu_{ef}\sqrt{g}, \mu_{ef}\sqrt{g}, \lambda_{ef}\sqrt{g}/C_p, \mu_t\sqrt{g}/\sigma_k, \mu_t\sqrt{g}/\sigma_\varepsilon]^{-1}. \tag{13}$$

Here v^1, v^2 and v^3 are the physical contravariant components of the velocity in the $\mathbf{e}_1$-, $\mathbf{e}_2$- and $\mathbf{e}_3$-direction respectively, g, g^{11}, g^{12}, g^{22}, g^{23}, g^{31} and g^{33} are the metric tensors and S_φ are the source terms expressed by curvilinear co-ordinates.

The discretized equations are obtained by integrating (11) over the appropriate control volumes and expressed in terms of neighbouring grid point values. In the present method a pressure correction equation is used instead of the continuity equation.

SOLUTION PROCEDURE

The discretized equations of (11) are solved by using the pressure correction method. A central difference approximation is used for all diffusion terms and an upwinding scheme is used for convection terms. Figure 1 shows the control volume with a central point P surrounded by neighbouring grid points E, W, S and N. This control volume is used for calculating all scalar variables, including the correction pressure, the total enthalpy, the turbulent kinetic energy and its dissipation rate. The control volumes for solving the momentum equations are shown in Figure 2. All the discretized equations are solved by successive iterations with the linear relaxation method.[24] No additional artificial viscosity is required for the present solution

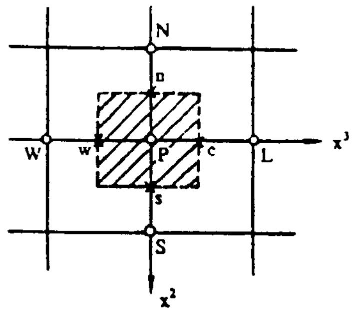

Figure 1. Control volume for solving scalar variables

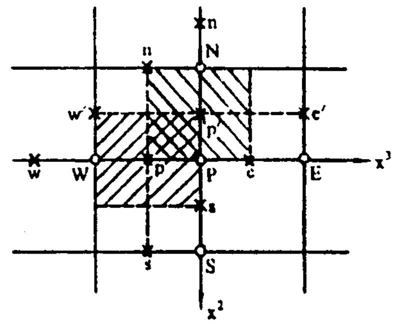

Figure 2. Control volume for solving momentum equations

procedure. For a three-dimensional flow calculation the control volumes are similar to the two-dimensional ones.

Introducing the velocity correction terms into the continuity equation, the pressure correction equation can be obtained and expressed by the following discretized form:

$$a_{\mathrm{P}} p'_{\mathrm{P}} = \sum_I a_I p'_I + S_{p'} \quad (I = \mathrm{E, W, S, N, U, D}). \tag{14}$$

Because this equation is solved by the linear relaxation method, it may be rewritten as

$$-a_{\mathrm{N}} p'_{\mathrm{N}} + a_{\mathrm{P}} p'_{\mathrm{P}} - a_{\mathrm{S}} p'_{\mathrm{S}} = N_{p'}, \tag{15}$$

where the differential coefficients a_{N}, a_{P} and a_{S} and the right-hand $N_{p'}$ term are determined from the previous iteration. This equation is solved for correcting the pressure and velocity field.

For all scalar variables, such as I, k and ε, the discretized equations are given by

$$-a_{\mathrm{N}} \varphi_{\mathrm{N}} + a_{\mathrm{P}} \varphi_{\mathrm{P}} - a_{\mathrm{S}} \varphi_{\mathrm{S}} = N_{\varphi}, \tag{16}$$

where φ represents one of the scalar variables.

Then the difference equations for the velocities are

$$a_{\mathrm{p}} \varphi_{\mathrm{p}} = \sum_i a_i \varphi_i + S_{\varphi} \quad (i = \mathrm{e, w, s, n, u, d}) \tag{17}$$

or

$$-a_{\mathrm{n}} \varphi_{\mathrm{n}} + a_{\mathrm{p}} \varphi_{\mathrm{p}} - a_{\mathrm{s}} \varphi_{\mathrm{s}} = N_{\varphi}, \tag{17a}$$

where φ denotes one of the variables.

Throughout the near-wall regions the wall function together with the k–ε turbulence model is employed so as to reduce the number of grid points.

The time difference between two iteration steps depends on the local Mach number and grid sizes, etc. In the present method it is taken to be 10^{-5}–10^{-3}. The final convergence is decided by a residual source criterion.

COMPUTATIONAL RESULTS

Axisymmetric gas turbine diffuser

The method has been used to study an axisymmetric gas turbine diffuser. The inlet Mach number is 0·3 and the Reynolds number, based on the inlet parameters and the mean diameter, is $8{\cdot}59 \times 10^6$. The grid size is 97×53 nodes. The grid system generated is shown in Figure 3. The diffuser has its form shown by IEE'I'. For a careful treatment of the outlet boundary condition the additional number of grid points is adopted. Then the whole flow field, including three

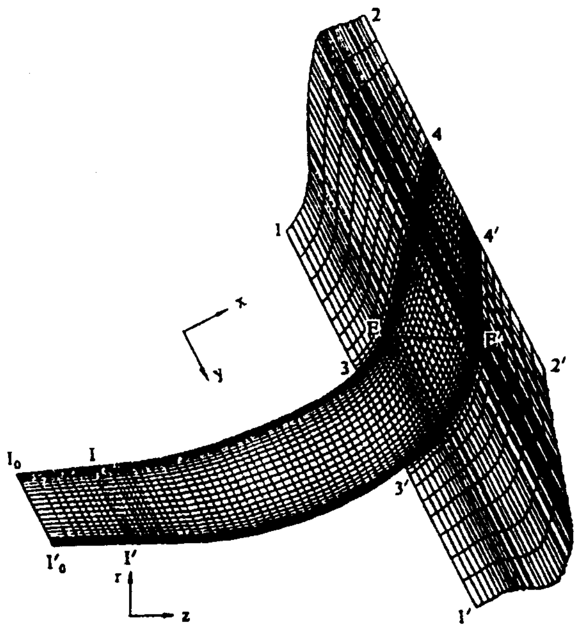

Figure 3. Computational grid system of a diffuser

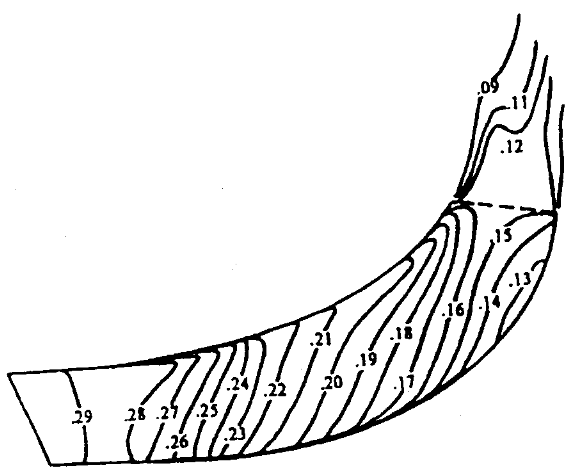

Figure 4. Contour of Mach number in diffuser

additional computational domains 124E3, 1′2′4′E′3′ and E44′E′, is solved together with the diffuser. At the inlet boundary I_0I_0' the distributions of total pressure, total temperature and velocity are given. No-slip and no-flux conditions are applied on the solid walls $I_0$3E, I_0'3′E′, 3E and 3′E′. On the walls the turbulent kinetic energy and its dissipation rate are also assumed to be zero. At the outlet boundary 244′2′ the first derivative of all parameters along the x^3-direction is taken to be zero. At the boundaries 31, 12, 3′1′ and 1′2′ zero velocity is taken and the pressure, total enthalpy, temperature, turbulent kinetic energy and its dissipation rate are imposed to be uniform.

The numerical computational results are shown in Figures 4–6. The distributions of Mach number and static pressure are plotted in Figures 4 and 5 respectively, while the velocity vectors

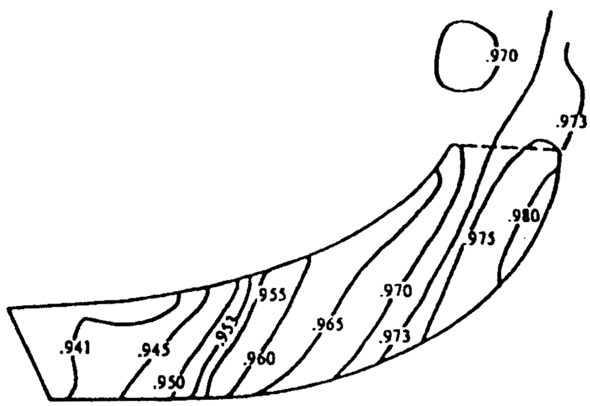

Figure 5. Contour of static pressure in diffuser

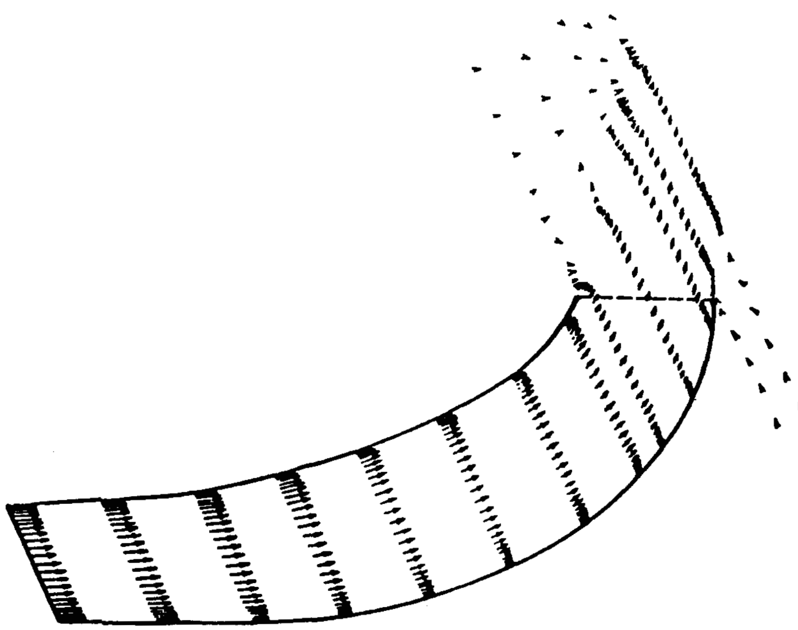

Figure 6. Velocity vectorgram in diffuser

are plotted in Figure 6. As shown in Figure 6, there are two vortexes beyond both the upper and lower sides of the jet flow from the diffuser in the outside space.

2D compressor blade cascade[25]

The solidity is 1·52. The inlet and outlet flow angles are $-30°$ and $13{\cdot}09°$ respectively. The inlet Mach number is 0·305. The computational grid system with the number of grid points of 99×24 nodes is shown in Figure 7. The upstream and downstream regions are calculated together with the flow field in the blade channel. In these two regions the periodicity condition is applied. The grid points are distributed non-uniformly along the circumferential direction. Refinement of the grid system is required near both the pressure and suction surfaces. The comparison between the calculated and experimental results is shown in Figure 8. In Figures 9 and 10 the velocity vectorgram and Mach number distribution are plotted respectively. The velocity distribution along the circumferential direction at the 80th axial station is shown in Figure 11.

3D flow in a turbine cascade[12]

For verification, predictions for a turbine cascade are compared with three-dimensional measured data.[12] The present calculation is carried out by using a body-fitted co-ordinate system as used in the previous examples and its data are interpolated into the normal sections by numbers 1–3 shown in Figure 12. Because of the symmetry of the blade, only half of the blade is treated and the number of grid points along the blade height is 19 nodes. The grid size used here is $64 \times 24 \times 19$ nodes. Figures 13 and 14 show the distributions of the longitudinal mean kinetic energy coefficients calculated and measured respectively. Figures 15 and 16 illustrate the velocity vectorgrams of the predicted and measured results respectively at the same normal sections.

CONCLUSIONS

A code to study internal turbulent flow problems has been developed. The code has been used to simulate the motion of axisymmetric diffuser, two-dimensional cascade and three-dimensional cascade flows. Numerical results were compared with experimental data. The agreement was

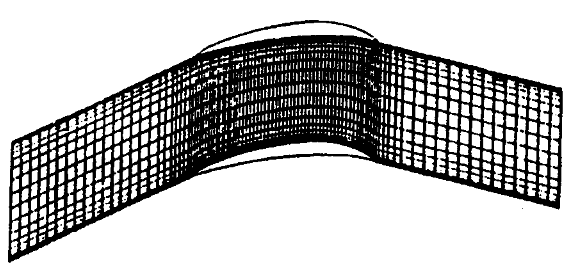

Figure 7. Grid system of a compressor blade cascade

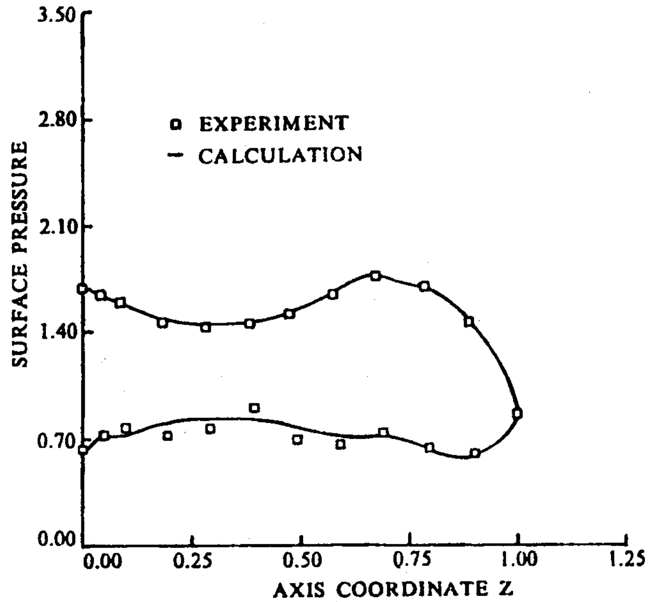

Figure 8. Comparison between experimental and calculated results

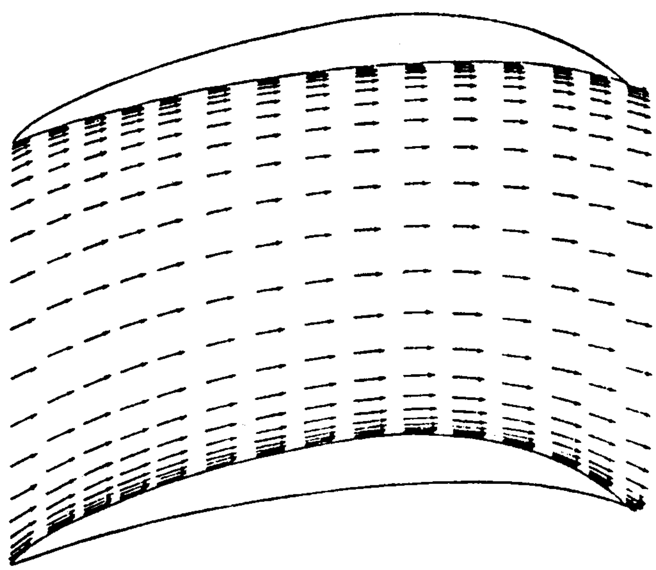
Figure 9. Velocity vectorgram of a compressor blade cascade flow field

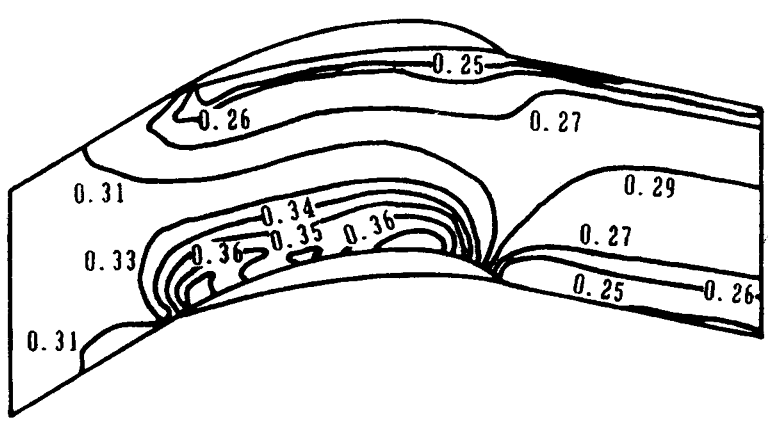

Figure 10. Mach number distribution of a compressor blade cascade flow field

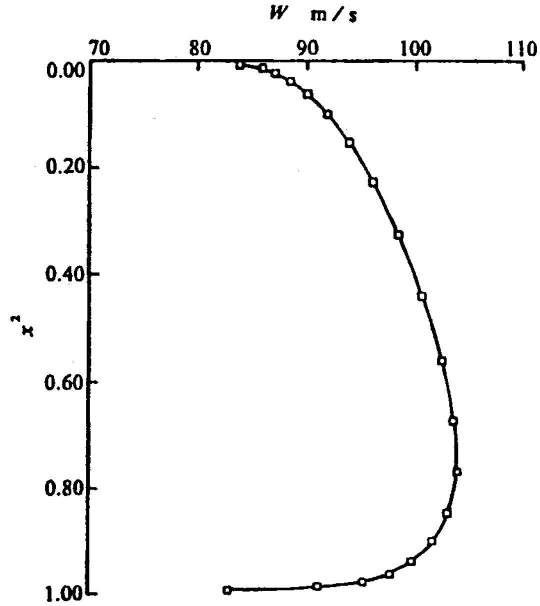

Figure 11. The circumferential velocity distribution at the 80th station

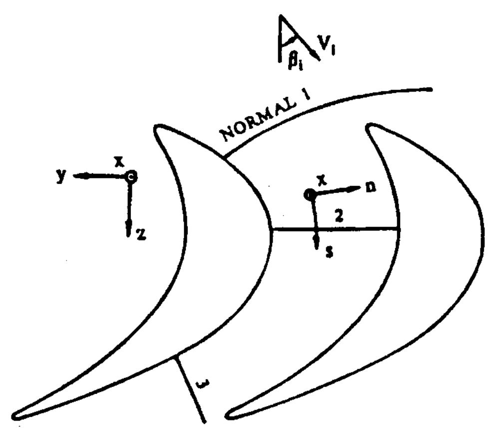

Figure 12. Cascade geometry and its normal surfaces

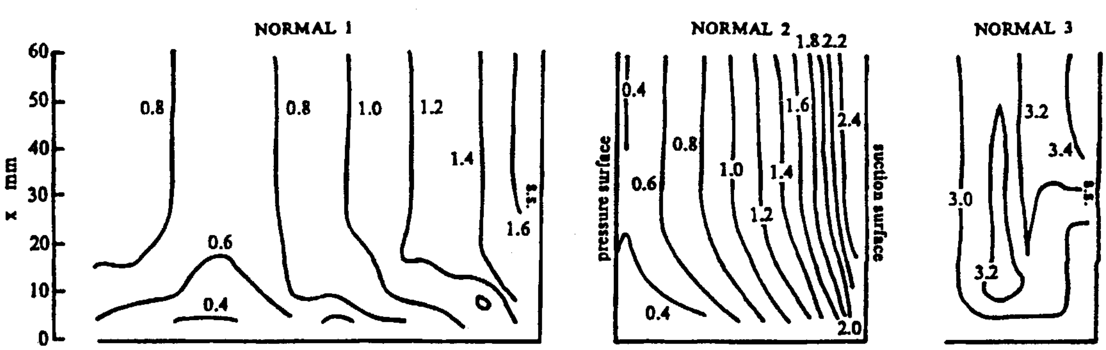

Figure 13. Distribution of calculated longitudinal mean kinetic energy coefficient

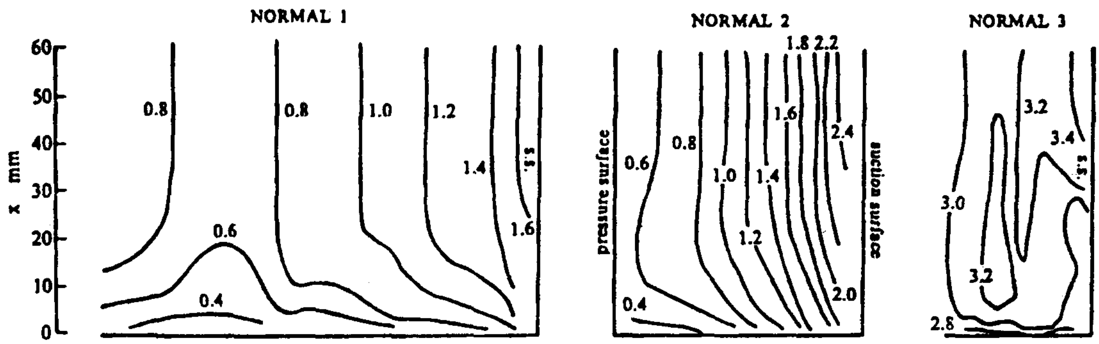

Figure 14. Distribution of measured longitudinal mean kinetic energy coefficient

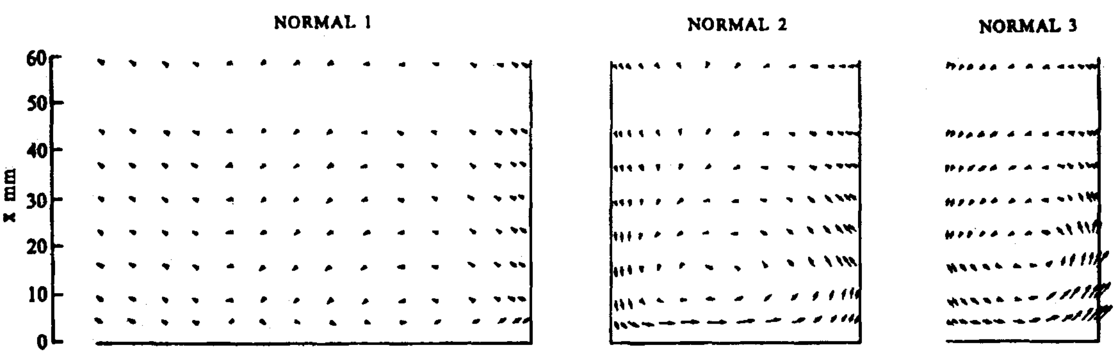

Figure 15. Velocity vectorgram of predicted results

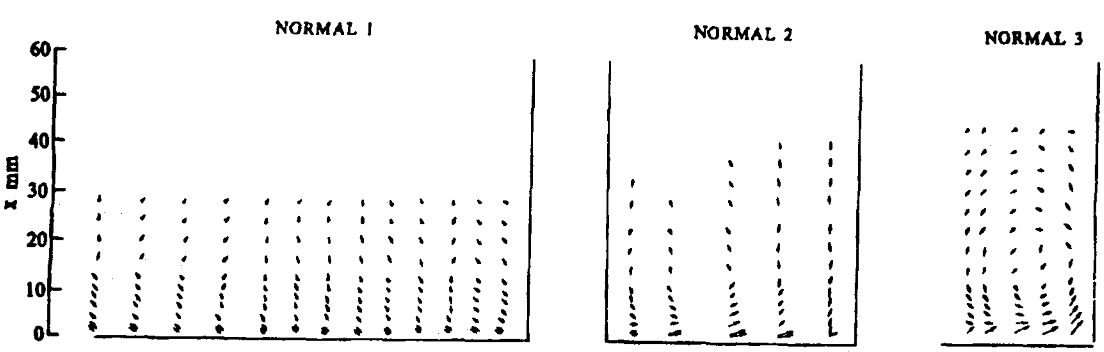

Figure 16. Velocity vectorgram of measured results

found to be good, showing that this code can be used as a tool for simulating and analysing two- and three-dimensional internal turbulence phenomena.

APPENDIX: NOMENCLATURE

C_1, C_2, C_μ	empirical constants in turbulence model
C_p	specific heat at constant pressure
$\mathbf{F}_{vis}$	viscous vector
g, g^{ij}	metric tensors
G	generation rate of turbulent kinetic energy
I	total enthalpy
k	turbulent kinetic energy
p	static pressure
Pr	laminar Prandtl number
Pr_t	turbulent Prandtl number
$\dot{q}$	heat transfer term
R	gas constant
S	source term
t	time
T	static temperature
v^j	physical contravariant components of velocity
$\mathbf{V}$	absolute velocity vector
V_r, V_ϕ, V_z	velocity components in cylindrical co-ordinates
x^j	general curvilinear co-ordinates

Greek symbols

Γ	generalized diffusion coefficient
ε	turbulent energy dissipation rate
λ	conductive coefficient
μ_{ef}	effective viscosity
μ_l	laminar viscosity
μ_t	turbulent viscosity
ρ	static density
$\sigma_k, \sigma_\varepsilon$	empirical constants in turbulence model
φ	generalized dependent variable
Φ	dissipation function

Subscript

φ	corresponding to generalized dependent variable

Superscript

	correction value

REFERENCES

1. D. G. Gregory-Smith and C. P. Graves, 'Secondary flows and losses in a turbine cascade', *AGARD CP 351*, 1983.
2. P. Zunino, M. Ubaldi and A. Satta, 'Measurements of secondary flows and turbulence in a turbine cascade passage', *ASME Paper 87-GT-132*, 1987.

3. N. T. Birch, 'Navier–Stokes predictions of transition, loss and heat transfer in a turbine cascade', *ASME Paper 87-GT-22*, 1987.
4. I. Khalil, W. Tabakoff and A. Hamed, 'Viscous flow analysis in mixed flow rotors', *J. Eng. Power*, **102**, 193–201 (1980).
5. Chen Naixing and Zhang Fengxian, 'A comparison between full and simplified Navier–Stokes equation solution for rotating blade cascade flow on S_1 stream surface of revolution', *ASME Paper 85-GT-4*, 1985.
6. Chen Naixing, Zhang Fengxian and Li Weihong, 'An inverse (design) problem solution method for the blade cascade flow on stream surface of revolution', *ASME Paper 86-GT-159*, 1986.
7. O. Key Kwon, 'Navier–Stokes solution for steady two dimensional transonic cascade flows', *ASME Paper 87-GT-54*, 1987.
8. S. Yamamoto, H. Daiguji and K. Ito, 'Computation of transonic cascade flow using the Euler and Navier–Stokes equation of contravariant velocities', *IGTC 39*, Tokyo, 1987, Paper 87.
9. B. C. Weinberg, R. J. Yang, H. McDonald and S. J. Shamroth, 'Calculations of two- and three-dimensional transonic cascade flow fields using Navier–Stokes equations', *ASME Paper 85-GT-66*, 1985.
10. B. E. Wake, L. N. Sankar and J. Wu, 'An efficient procedure for the numerical solution of three-dimensional viscous flows', *ISABE Paper 87-1159*, 1987.
11. C. Hah, 'A Navier–Stokes analysis of three-dimensional flow inside turbine blade row at design and off-design condition', *J. Eng. Gas Turb. Power*, **106**, 421–429 (1984).
12. J. Moore, J. G. More and D. H. Timmis, 'Performance evaluation of centrifugal compressor impellers using three-dimensional viscous flow calculations', *J. Eng. Gas Turb. Power*, **106**, 475–481 (1984).
13. M. Pouagare and R. A. Delaney, 'Study of three-dimensional viscous flows in an axial compressor cascade including tip leakage effects using a SIMPLE-based algorithm', *J. Turbomach.*, **108**, 51–58 (1986).
14. S. V. Patankar and D. B. Spalding, 'A calculation procedure for heat, mass and momentum transfer in three-dimensional parabolic flows', *Int. J. Heat Mass Transfer*, **15**, 1787–1806 (1972).
15. A. M. Abdelmeguid, N. C. Markatos, K. Muraoka and D. B. Spalding, 'A comparison between the parabolic and partially-parabolic solution procedure for three-dimensional turbulent flows around ships' hulls', *Appl. Math. Model.*, **3**, 249–258 (1979).
16. I. M. Khalil and H. G. Weber, 'Modelling of three-dimensional flow in turning channels', *Trans. ASME*, **106**, 682–691 (1984).
17. W. Shyy, S. S. Tong and S. M. Correa, 'Numerical recirculating flow calculation using a body-fitted coordinate system', *Numer. Heat Transfer*, **8**, 99–113 (1985).
18. B. L. Lapworth and R. L. Elder, 'Computation of the jet wake flow structure in a low speed centrifugal impeller', *ASME Paper 88-GT-247*, 1988.
19. C. Hah, 'Numerical solution of three-dimensional turbulent flows for modern gas turbine components', *ASME Paper 87-GT-84*, 1987.
20. Chen Naixing and Zhang Fengxian, 'A full Navier–Stokes solution of viscous gas flow through profile cascade or S_1 stream surface of revolution employing non-orthogonal curvilinear system', *Sci. Sinica, Ser. A*, **27**(8), 1112–1120 (1984).
21. B. E. Launder and D. B. Spalding, 'The numerical computational of turbulent flows', *Comput. Methods Appl. Mech. Eng.*, **3**, 269–289 (1974).
22. S. V. Patankar and D. B. Spalding, *Heat and Mass Transfer in Boundary Layers*, 2nd edn, London, 1970.
23. Chen Naixing, 'Some problems in viscous gas flow in turbomachinery: viscous and heat-transfer terms and methods for solution of basic equations', *Sci. Sinica, Ser. A*, **27**, 648–661 (1983).
24. Xu Yanji and Chen Naixing, 'Numerical computation of 2D viscous flow field through turbomachinery cascades', *Paper IET 89-ADT-1*, Institute of Engineering Thermophysics, Chinese Academy of Sciences, 1989.
25. M. Savage, A. R. Felix and J. C. Emery, 'High-speed cascade tests of a blade section designed for typical hub conditions of high-flow transonic rotors', *NACA RM L55F07*, 1955.